

Maximum Power Point Tracking using Sliding Mode Control for Photovoltaic Array

J. Ghazanfari* and M. M. Farsangi**

Abstract: In this paper, a robust Maximum Power Point Tracking (MPPT) for PV array has been proposed using sliding mode control by defining a new formulation for sliding surface which is based on increment conductance (INC) method. The stability and robustness of the proposed controller are investigated to load variations and environment changes. Three different types of DC-DC converter are used in Maximum Power Point (MPP) system and the results obtained are given. The simulation results confirm the effectiveness of the proposed method in the presence of load variations and environment changes for different types of DC-DC converter topologies. In addition, a Model Predictive Control (MPC) is adopted from the literature to show the effectiveness of the proposed controller.

Keywords: Maximum Power Point Tracking, MPC, MPPT, Photovoltaic Array, Sliding Mode Control, SMC, Solar Cell.

1 Introduction

Photovoltaic generators have a nonlinear voltage-current characteristic with a unique Maximum Power Point (MPP), which depends on the temperature and irradiance condition. When these conditions are changed, the operating point and MPP will be changed. Therefore, MPPT control method is required to ensure that the maximum available power is obtained from the panel. A review on maximum power point tracking control techniques is given in [1].

Different approaches have been reported in literature such as look up table method [2, 3], hill-climbing [4-6], Perturb & Observe (P&O) method [7, 8], improved P&O [9, 10], increment conductance (INC) method [11-13], fuzzy based method [14, 15] proportional open-circuit voltage (or short-circuit current) [16], near-MPP operation [17], Neural-network [18], Model Predictive Control (MPC) [19], fractional order incremental conductance method [20] and heuristic algorithm by applying ant colony [21].

Also, the concept of sliding mode control is used to track the MPP in [22-25] where in some of these approaches the reference current is used for control law synthesis which may lead to a lack of robustness to operation conditions.

In this paper, a different sliding surface is defined and used for MPPT control. This surface is based on

INC method. INC method consists in using the slope of the derivative of the voltage with respect to the current in order to reach the maximum power point. Therefore, there is no need to use the current reference directly in the formulation. Also, the mathematical modeling is developed for different DC-DC converter topologies such as buck converter, boost converter and buck-boost converter.

By defining this sliding surface a robust approach is proposed in this paper. The robustness of the proposed approach is investigated in the presence of load variations and environment changes. Also, a Model Predictive Control (MPC) is adopted from the literature to show the effectiveness of the proposed controller. The obtained results show that the proposed controller performs better. The paper is organized as follow: the explanation about MPP system is given in section 2. The proposed sliding mode control approach for MPPT is described in section 3. The implementation and results are presented in section 4. The comparison of the proposed sliding model control (SMC) and the adopted MPC is made in section 5 and finally conclusion is drawn in section 6.

2 The PV System Configuration

The MPP system block diagram is shown in Fig. 1 which consists of PV array, DC/DC converter, the load such as battery array and controller where in this paper sliding mode controller based on INC method is used as a controller. More details about the characteristic of PV array, DC/DC converter and the sliding mode controller are given below.

Iranian Journal of Electrical & Electronic Engineering, 2013.

Paper first received 4 Sep. 2012 and in revised form 6 Apr. 2013.

* The Author is with Young Researchers Society, Shahid Bahonar University of Kerman, Kerman, Iran.

** The Author is with Electrical Engineering Department, Shahid Bahonar University of Kerman, Kerman, Iran.

E-mails: jaber.gh64@Gmail.com, mmaghfoori@uk.ac.ir.

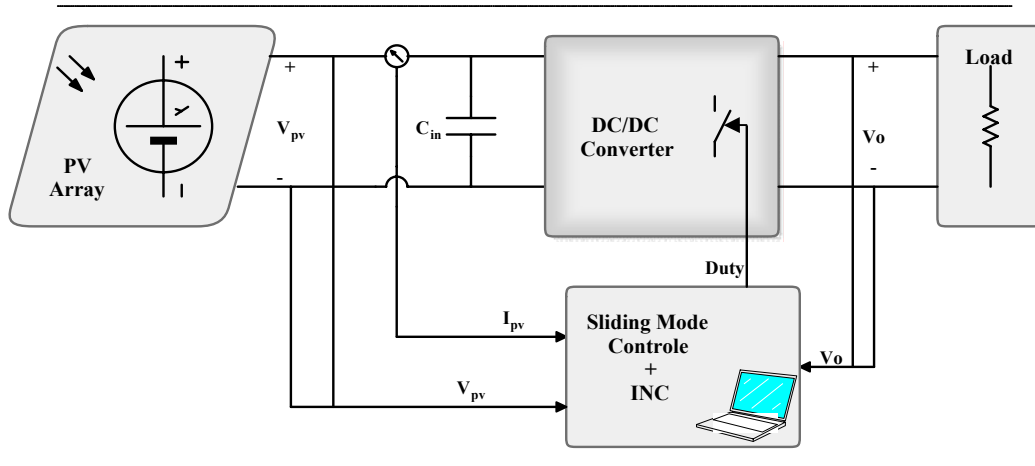


Fig. 1 MPPT system block diagram.

2.1 The Characteristics of PV Array

The double-diode model of PV cell is shown in Fig. 2. This model is commonly accepted as reflecting the behavior of polycrystalline silicon power cells [26]. One of the two diodes represents the diffusion current in the PN junction where as the other is added to take the space charge recombination effect into account. The mathematical expression of the equivalent model is given by the following Eq. (1).

$$I_{pv} = I_{ph} - I_{s1} \left\{ \exp \left(\frac{V_{pv} + R_s I_{pv}}{n_1 k T_c / q} \right) - 1 \right\} - \dots \dots I_{s2} \left\{ \exp \left(\frac{V_{pv} + R_s I_{pv}}{n_2 k T_c / q} \right) - 1 \right\} - \left(\frac{V_{pv} + R_s I_{pv}}{R_p} \right) \quad (1)$$

where I_{pv} and V_{pv} are the solar cell output current and voltage respectively, I_{s1} & I_{s2} are the dark saturation current, q is the charge of an electron, n_1 and n_2 are the diode quality (ideality) factor, K is the Boltzmann constant, T_c is the absolute temperature and R_s & R_p are the series and shunt resistances of the solar cell. R_s is the resistance offered by the contacts and the bulk semiconductor material of the solar cell. R_p is related to the non-ideal nature of the p-n junction and the presence of impurities near the edges of the cell that provide a short-circuit path around the junction [26]. Therefore, the output current-voltage characteristic of a PV panel can be expressed by Eq. (2), where n_p and n_s are the number of solar cells in parallel and series respectively [11].

$$I_{pv} = n_p I_{ph} - n_p I_{s1} \left\{ \exp \left(\frac{V_{pv}/n_s + R_s I_{pv}/n_p}{n_1 k T_c / q} \right) - 1 \right\} - \dots \dots n_p I_{s2} \left\{ \exp \left(\frac{V_{pv}/n_s + R_s I_{pv}/n_p}{n_2 k T_c / q} \right) - 1 \right\} - n_p \left(\frac{V_{pv}/n_s + R_s I_{pv}/n_p}{R_p} \right) \quad (2)$$

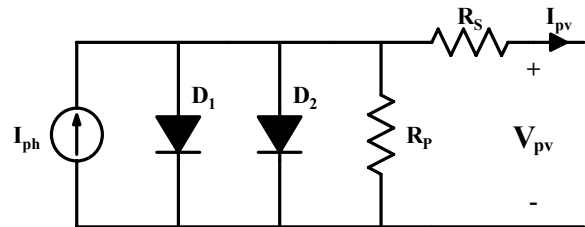


Fig. 2 Equivalent circuit model of PV.

The irradiation and the temperature are two important factors that strongly affect the characteristics of solar modules. The electrical parameters (I_{s1} , I_{s2} , I_{ph} , n_1 , n_2 , R_s , R_p) change if temperature and solar irradiance change. The mathematical expression of the dependent the electrical parameters on the temperature (T_c) and solar radiation (S) can be written as follows [27]:

$$I_{ph}(S) = I_{ph} \times \left(\frac{S}{S_{ref}} \right) \quad (3)$$

$$I_{ph}(T_c) = I_{ph} \{ 1 + T_{pi}(T_c - T_m) \}$$

$$R_s(T_c) = R_s \times \left(\frac{T_c}{T_m} \right)^{T_{rs}}, R_p(T_c) = R_p \times \left(\frac{T_c}{T_m} \right)^{T_{rp}} \quad (4)$$

$$I_{si}(T_c) = I_{si} \left(\frac{T_c}{T_m} \right)^{C_i} \times \exp \left\{ E_g \left(\frac{T_c}{T_m} - 1 \right) / n_i V_t \right\} \quad (5)$$

$$C_i = T_{si} / n_i, \quad i=1,2.$$

Fig. 3 shows the I-V and P-V characteristic curve of a solar array for different irradiance (600, 800 and 1000 W/m²) at a fixed array temperature (25°C). As it is evident in Fig. 3, the irradiation and the temperature are two important factors that highly affect the characteristics of solar modules. Therefore, MPP must constantly be tracked to ensure that the PV generation system achieves the maximum power output in real time.

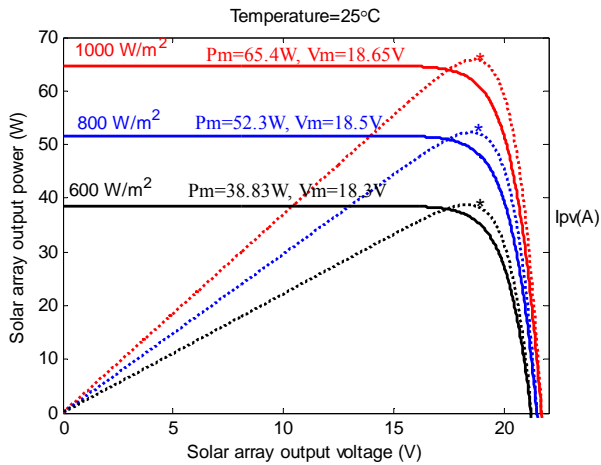


Fig. 3 PV cell characteristic under different irradiance (W/m^2) level.

2.2 Converters Topology

DC/DC Converters are most widely applied in photovoltaic systems as an intermediate between the solar cells and the load to pursue the maximum power point (MPPT). Different topologies and different design approaches could be used for DC/DC converters. In this study three different models of converters such as buck, boost and buck-boost converters are used. The diagrams in Figs. 4-6 show the structure of these converters with the switching period of T and duty cycle d.

For each converter, state equation of voltage results in the Eqs. (6)-(8).

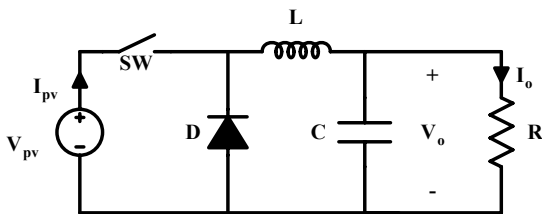


Fig. 4 DC/DC buck converter.

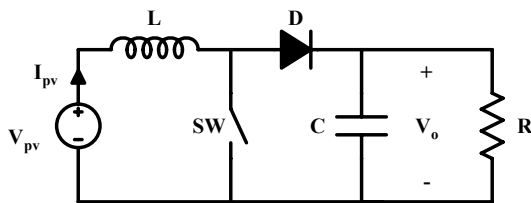


Fig. 5 DC/DC boost converter.

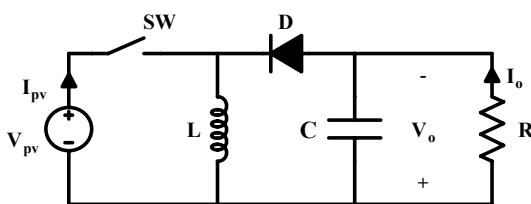


Fig. 6 DC/DC buck-boost converter.

$$\frac{dI_L}{dt} = -\frac{1}{L}V_o + \frac{d}{L}V_{pv} \quad \text{Buck converter} \quad (6)$$

$$\frac{dI_L}{dt} = -\frac{1-d}{L}V_o + \frac{1}{L}V_{pv} \quad \text{Boost converter} \quad (7)$$

$$\frac{dI_L}{dt} = -\frac{1-d}{L}V_o + \frac{d}{L}V_{pv} \quad \text{Buck-boost converter} \quad (8)$$

Also, the relation between I_L and I_{pv} for each type of converter is as follows:

$$I_L = K \cdot I_{pv} \quad (9)$$

in which, K is given as follows:

$$K = \begin{cases} 1/d, & \text{for buck converter} \\ 1, & \text{for boost converter} \\ 1/d, & \text{for buck-boost converter} \end{cases} \quad (10)$$

3 The Proposed Sliding Mode Control Approach for MPPT

The sliding mode control consists of two steps. In the first step, an equilibrium surface is designed and in the second step, a discontinuous control law will be designed. In this paper, the sliding surface is defined based on INC method. INC method consists in using the slope of the derivative of the voltage with respect to the current in order to reach the maximum power point. In INC method, the MPP is calculated by solving Eq. (11):

$$\frac{\partial P_{pv}}{\partial V_{pv}} = \frac{\partial (V_{pv} \cdot I_{pv})}{\partial V_{pv}} = V_{pv} \cdot dI_{pv} + dV_{pv} \cdot I_{pv} = 0 \quad (11)$$

where I_{pv} and V_{pv} are the PV current and voltage, respectively. This equation shows that to obtain this point, $(-dV_{pv}/dI_{pv})$ must be equal to (V_{pv}/I_{pv}) . In INC method, $(-dV_{pv}/dI_{pv})$ is known as instantaneous array resistance (R) and (V_{pv}/I_{pv}) is known as incremental resistance (r). Fig. 7 shows the I-V characteristic curve of a solar array under $800W/m^2$ irradiance at $25^\circ C$ using INC method.

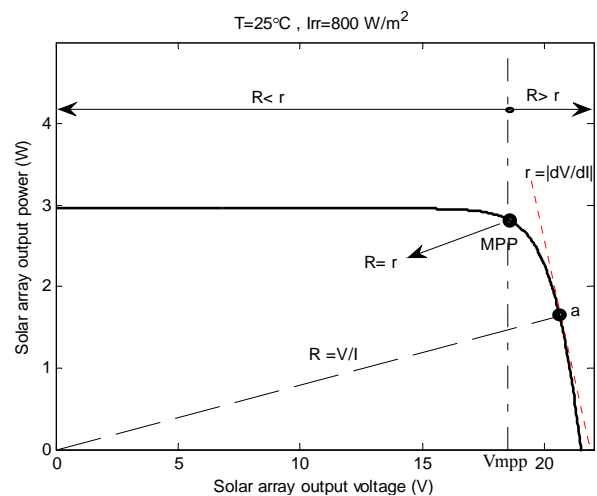


Fig. 7 I-V curve of PV array using INC method.

Thus, at maximum power point, the following equation must be satisfied as shown in Fig. 7:

$$\frac{V_{pv}}{I_{pv}} = \frac{dV_{pv}}{dI_{pv}} \rightarrow R(I_{pv}) - r(I_{pv}) = 0 \quad (12)$$

Therefore, the sliding surface can be defined based on the error between the instantaneous array resistance (R) and the incremental resistance (r):

$$\sigma = R(I_{pv}) - r(I_{pv}) \quad (13)$$

Now by defining the above surface, control law should be obtained for three different of converters topologies that forces the system to move on the sliding mode surface in a finite time in which the following structure for control input is used as it is used in [25]:

$$u(t) = u_{eq}(t) + u_n(t) \quad (14)$$

where u_{eq} defines the system's behavior on the sliding surface and known as equivalent control-input and u_n known as non-linear switching input that moves the state to the sliding surface and keeps the state on the sliding surface in the presence of the uncertainty. u_{eq} is obtained from the invariance condition and is given as below:

$$(\sigma = 0, d\sigma = 0) \Leftrightarrow (u = u_{eq}) \quad (15)$$

For three types of converters the derivative of the sliding surface Eq. (13) is:

$$d\sigma = \left(\frac{\partial R}{\partial I_{pv}} - \frac{\partial r}{\partial I_{pv}} \right) \cdot \frac{dI_{pv}}{dt} \quad (16)$$

Substituting Eq. (9) into Eq. (16) results in:

$$d\sigma = A \cdot \frac{dL}{dt} \quad (17)$$

where:

$$A = K \cdot \left(\frac{\partial R}{\partial I_{pv}} - \frac{\partial r}{\partial I_{pv}} \right) \quad (18)$$

By substituting Eqs. (6), (7) and (8) into Eq. (17), the time derivative of sliding surface is obtained for three different types of converters:

$$d\sigma = \begin{cases} A \cdot \left[u(t) \cdot \frac{V_{pv}}{L} - \frac{V_o}{L} \right] & \text{buck} \\ A \cdot \left[\frac{V_{pv}}{L} - (1-u(t)) \cdot \frac{V_o}{L} \right] & \text{boost} \\ A \cdot \left[u(t) \cdot \frac{V_{pv}}{L} - (1-u(t)) \cdot \frac{V_o}{L} \right] & \text{buck-boost} \end{cases} \quad (19)$$

Considering Eq. (19) and Eq. (15), the equivalent control-input is obtained as:

$$u_{eq}(t) = \begin{cases} \left(\frac{V_o}{V_{pv}} \right) & \text{buck} \\ \left(1 - \frac{V_{pv}}{V_o} \right) & \text{boost} \\ \left(\frac{V_o}{V_o + V_{pv}} \right) & \text{buck-boost} \end{cases} \quad (20)$$

Now $u_n(t)$ is chosen so that the Lyapunov stability criteria ($d\sigma \cdot \sigma < 0$) is met.

The chosen $u_n(t)$ is as:

$$u_n(t) = \begin{cases} \left(-\frac{V_o}{V_{pv}} + \frac{1}{M} \right) & \text{buck} \\ \left(\frac{V_{pv}}{V_o} + M \right) & \text{boost} \\ \left(\frac{-V_o}{V_o + V_{pv}} + \frac{1}{(1+M)} \right) & \text{buck-boost} \end{cases} \quad (21)$$

where M is control signal which is calculated through Lyapunov stability criteria (given below). Therefore, the Eqs. (20), (21) give the control law defined in Eq. (14) as:

$$u(t) = \begin{cases} \frac{1}{M} & \text{buck} \\ 1-M & \text{boost} \\ \frac{1}{(1+M)} & \text{buck-boost} \end{cases} \quad (22)$$

A Lyapunov function and its time derivative are defined as:

$$V = \frac{1}{2} \sigma^2, \quad dV = d\sigma \cdot \sigma \quad (23)$$

If Eq. (19) is substituted into Eq. (22), we get:

$$dV = \begin{cases} A \cdot \left[u(t) \cdot \frac{V_{pv}}{L} - \frac{V_o}{L} \right] \cdot \sigma & \text{buck} \\ A \cdot \left[\frac{V_{pv}}{L} - (1-u(t)) \cdot \frac{V_o}{L} \right] \cdot \sigma & \text{boost} \\ A \cdot \left[u(t) \cdot \frac{V_{pv}}{L} - (1-u(t)) \cdot \frac{V_o}{L} \right] \cdot \sigma & \text{buck-boost} \end{cases} \quad (24)$$

Substituting Eq. (22) into Eq. (24) gives the following result for three different types of converters:

$$dV = \left(\frac{A}{L} \right) \cdot [V_{pv} - M \cdot V_o] \cdot \sigma \quad (25)$$

Assume the operating point of the system is 'a' in Fig. 7. Since the gradient is negative, moving the operating point to the right side causes increasing in the current of PV array, which results in decreasing of R and increasing of r , therefore, ($\partial R / \partial I_{pv} < 0$, $\partial r / \partial I_{pv} > 0$).

Also, moving the operating point to the left side causes decreasing in the current of PV array, which results in increasing of R and decreasing of r , therefore, ($\partial R / \partial I_{pv} < 0$, $\partial r / \partial I_{pv} > 0$). Thus, the sign of A in Eq. (24) is always negative. Based on Eq. (12) and Eq. (13), for positive sliding surface we have:

$$\sigma > 0 \rightarrow \frac{V_{pv}}{I_{pv}} > \left| \frac{dV_{pv}}{dI_{pv}} \right| \quad (26)$$

For a positive parameter α , we have:

$$\sigma > 0 \rightarrow \left(\frac{V_{pv}}{I_{pv}} \right)^\alpha > \left| \frac{dV_{pv}}{dI_{pv}} \right|^\alpha \quad (27)$$

Multiplying above inequality in $\frac{(V_{pv})^{(1-\alpha)} \cdot (I_{pv})^\alpha}{V_o} > 0$ results in:

$$\sigma > 0 \rightarrow \left(\frac{(V_{pv})^{(1-\alpha)} \cdot (I_{pv})^\alpha}{V_o} \right) \left(\frac{V_{pv}}{I_{pv}} \right)^\alpha > \left(\frac{(V_{pv})^{(1-\alpha)} \cdot (I_{pv})^\alpha}{V_o} \right) \left| \frac{dV_{pv}}{dI_{pv}} \right|^\alpha \quad (28)$$

which simplifies as:

$$\sigma > 0 \rightarrow \left(\frac{V_{pv}}{V_o} \right) > \left(\frac{(V_{pv})^{(1-\alpha)} \cdot (I_{pv})^\alpha}{V_o} \right) \left| \frac{dV_{pv}}{dI_{pv}} \right|^\alpha \quad (29)$$

Similar to $\sigma > 0$, for $\sigma < 0$ we get:

$$\sigma < 0 \rightarrow \left(\frac{V_{pv}}{V_o} \right) < \left(\frac{(V_{pv})^{(1-\alpha)} \cdot (I_{pv})^\alpha}{V_o} \right) \left| \frac{dV_{pv}}{dI_{pv}} \right|^\alpha \quad (30)$$

Based on Eqs. (29)-(30), the control law M can be chosen as:

$$M = \left(\frac{(V_{pv})^{(1-\alpha)} \cdot (I_{pv})^\alpha}{V_o} \right) \left| \frac{dV_{pv}}{dI_{pv}} \right|^\alpha \quad (31)$$

Therefore, for positive and negative sliding surface we have:

$$\sigma > 0 \rightarrow \left(\frac{V_{pv}}{V_o} \right) > M \rightarrow [V_{pv} - M \cdot V_o] > 0 \rightarrow \sigma \cdot [V_{pv} - M \cdot V_o] > 0$$

$$\sigma < 0 \rightarrow \left(\frac{V_{pv}}{V_o} \right) < M \rightarrow [V_{pv} - M \cdot V_o] < 0 \rightarrow \sigma \cdot [V_{pv} - M \cdot V_o] > 0 \quad (32)$$

By considering Eq. (32) and since $A < 0$, the time derivative of Lyapunov function in Eq. (25) is negative ($dV = d\sigma \cdot \sigma < 0$). Thus, by substituting Eq. (31) into Eq. (22), the control input is obtained as follows which forces the system to move on the sliding mode surface in a finite time:

$$u(t) = \begin{cases} \left(\left(\frac{(V_{pv})^{(1-\alpha)} \cdot (I_{pv})^\alpha}{V_o} \right) \left| \frac{dV_{pv}}{dI_{pv}} \right|^\alpha \right)^{-1} & \text{buck} \\ 1 - \left(\frac{(V_{pv})^{(1-\alpha)} \cdot (I_{pv})^\alpha}{V_o} \right) \left| \frac{dV_{pv}}{dI_{pv}} \right|^\alpha & \text{boost} \\ \left(1 + \left(\frac{(V_{pv})^{(1-\alpha)} \cdot (I_{pv})^\alpha}{V_o} \right) \left| \frac{dV_{pv}}{dI_{pv}} \right|^\alpha \right)^{-1} & \text{buck-boost} \end{cases} \quad (33)$$

Since the range of duty cycle must lie in $0 < d < 1$, the real control signal for three different types of converters is proposed as:

$$d = \begin{cases} 0, & u(t) \leq 0 \\ u(t), & 0 < u(t) < 1 \\ 1, & 1 \leq u(t) \end{cases} \quad (34)$$

4 Implementation and Results

Fig. 1 is implemented in Matlab/Simulink by considering a PV power source by delivering a

maximum 65 W power, three types of converter models, and the proposed MPPT approach. The specification of the system is given in Tables 1, 2. The proposed MPPT is designed by sliding mode control and its robustness to irradiance, and load is investigated. To show the robustness, different operating points are used by considering different values of irradiance and load.

The tracking results with step irradiance input when it changes from 1000 to 600 and then to 800 W/m² under the same temperature and load are shown in Figs. 8-10 for three types of converters. The results obtained for three types of converters show that the system reaches steady state of irradiance levels very fast.

Also, the response of the system when is loaded heavily are shown in Figs. 11-13 for three types of converters. Figs. 11, 12 are the response of the system equipped with boost and buck-boost converters respectively, when the load is changed from 20 Ω to 100 Ω . Fig. 13 is the response of the system equipped with buck converter, when the load is changed from 5 Ω to 1 Ω .

Once again, the results obtained confirm the effectiveness of the proposed method in the presence of load variations for three types of converters.

Table 1 System specification.

Parameters	Value	Parameters	Value
n_1, n_2	1.4, 1.4	R_s, R_p	0.004, 5000 (Ω)
K	1.38×10^{-23} (J/K)	q	1.6×10^{-19} (C)
T	313 (K)	f	50 (KHz)
I_{sh}	3.7 (A)	V_{oc}	22 (v)
I_{s1}	1.02×10^{-6} (A)	I_{s2}	5.37×10^{-7} (A)
C_{in}	400 (μ F)	C	100 (μ F)

Table 2 The value of L and α for different converters.

Converter	L	α
Buck	5.5 (mH)	2
Boost	50 (μ H)	0.25
Buck-Boost	1.5 (mH)	1.5

5 Comparison

To show the effectiveness of the proposed method, a method is adopted from the literature [20]. This method is known as Fixed Step-Model Predictive Controller which is based on the modified INC algorithm. The main concept of the MPC technique is the prediction of the future behavior of the controlled variables. The criterion of the control method is expressed as a cost function to be minimized. To have a fair comparison, two controllers are designed for boost converter under the same condition which is reported in Table 3.

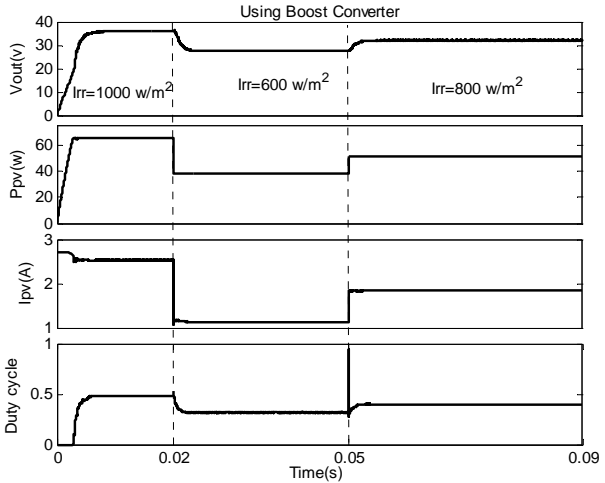


Fig. 8 Simulation with step irradiance change (1000-600-800 w/m^2), when the system is equipped with boost converter.

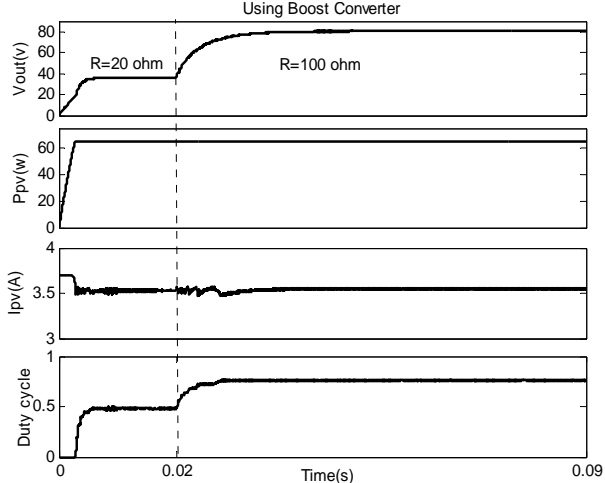


Fig. 11 Simulation with step load change (20Ω to 100Ω), when the system is equipped with boost converter.

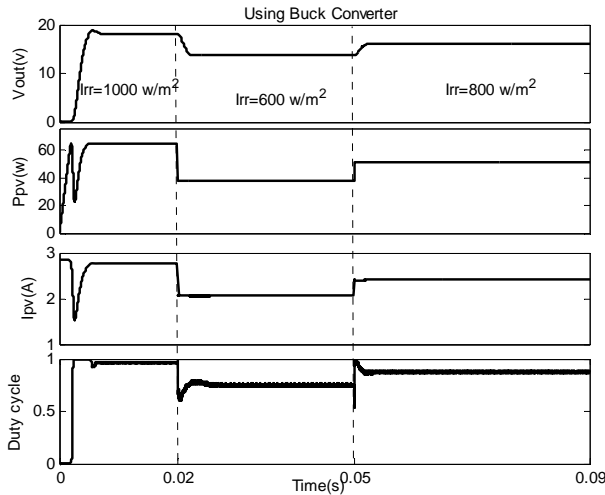


Fig. 9 Simulation with step irradiance change (1000-600-800 w/m^2), when the system is equipped with buck converter.

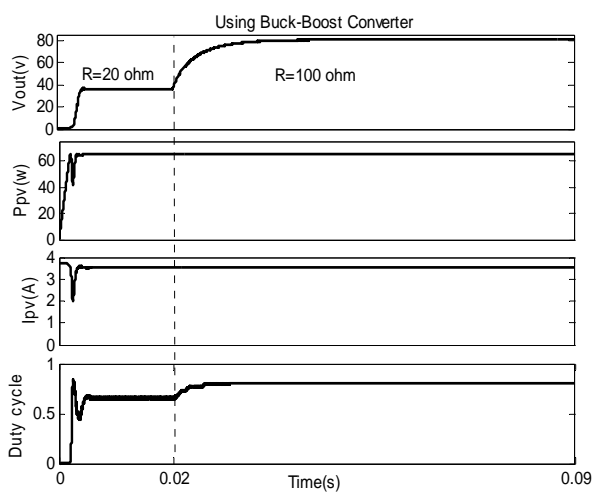


Fig. 12 Simulation with step load change (20Ω to 100Ω), when the system is equipped with buck-boost converter.

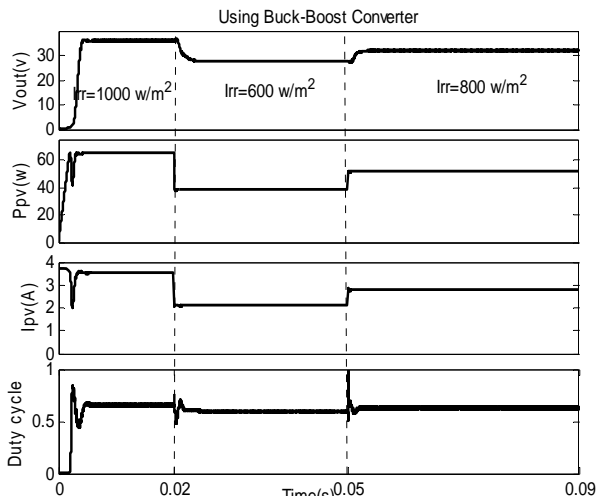


Fig. 10 Simulation with step irradiance change (1000-600-800 w/m^2), when the system is equipped with buck-boost converter.

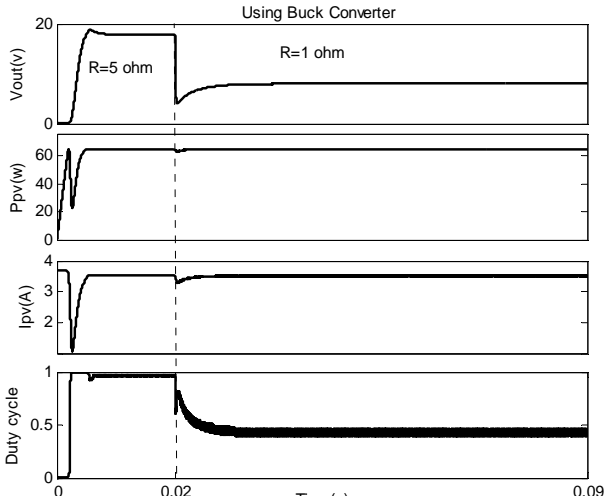


Fig. 13 Simulation with step load change (5Ω to 1Ω), when the system is equipped with buck converter.

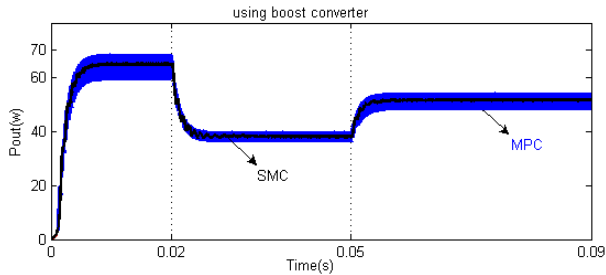


Fig. 14 Comparison of the proposed sliding model control (SMC) and the adopted MPC; with step irradiance change (1000-600-800 w/m²), when the system is equipped with boost converter.

Table 3 System specification for boost converter.

Parameters	Value
f	50 (KHz)
C _{in}	200 (μF)
L	0.5 (mH)
R	100 (Ω)
C	25 (μF)

The tracking results with step irradiance input when it changes from 1000 to 600 and then to 800 W/m² under the same temperature and load are shown in Fig. 14 for boost converter. This figure illustrates that under the same condition the proposed sliding mode control performs well while the proposed MPC is much oscillatory.

6 Conclusion

This paper presents an alternative approach for MPPT control using sliding mode control. The main contribution of the paper is defining a sliding surface which is based on INC method, using the slope of the derivative of the voltage with respect to the current in order to reach the maximum power point. Therefore, there is no need to use the current reference directly in the formulation. Also, the mathematical modeling is developed for different DC-DC converter topologies such as buck converter, boost converter and buck-boost converter. The robust performances of the system are checked for three types of converters in the presence of two types of disturbances; in the presence of step irradiance change and when the system is loaded heavily. The results obtained for three types of converters show that the system performs well and is robust to the variation of the external conditions. Furthermore, for the sake of comparison, a method is adopted from the literature which is known as Fixed Step-Model Predictive Controller (MPC). It is shown for boost converter that the proposed method is very effective in giving quality solutions consistently comparing to MPC.

References

- [1] Bhatnagar P. and Nema R. K., "Maximum power point tracking control techniques: State-of-the-art in photovoltaic applications Review Article", *Renewable and Sustainable Energy Reviews*, Vol. 23, pp. 224-241, July 2013.
- [2] Yamashita H., Tamahashi K., Michihira M., Tsuyoshi A., Amako K. and Park M., "A novel simulation technique of the PV generation system using real weather conditions", *In: Proceedings of the power conversion conference*, Vol. 2, pp. 839-844, Apr. 2002.
- [3] Park M. and Yu I. K., "A novel real-time simulation technique of photovoltaic generation systems using RTDS", *IEEE Trans Energy Convers*, Vol. 19, No. 1, pp. 164-169, March 2004.
- [4] Xiao W. and Dunford W. G., "A modified adaptive hill climbing MPPT method for photovoltaic power systems", *In: Proceedings of 35th Annual IEEE Power Electronics*, Vol. 3, pp. 1957-1963, June 2004.
- [5] Koutroulis E., Kalaitzakis K. and Voulgaris N. C., "Development of a microcontroller-based Photovoltaic maximum power point tracking control system", *IEEE Trans. Power Electron*, Vol. 16, No. 1, pp. 46-54, Jan. 2001.
- [6] Veerachary M., Senjyu T. and Uezato K., "Maximum power point tracking control of IDB converter supplied PV system", *IEE Proc. Electron. Power Appl.*, Vol. 148, No. 6, pp. 494-502, Nov. 2001.
- [7] Hua C. and Lin J., "An on-line MPPT algorithm for rapidly changing illuminations of solar arrays", *Renewable Energy*, Vol. 28, No. 7, pp. 1129-1142, June 2003.
- [8] Femia N., Petrone G., Spagnuolo G. and Vitelli M., "Optimization of perturb and observe maximum power point tracking method", *IEEE Trans. Power Electron*, Vol. 20, No. 4, pp. 963-973, July 2005.
- [9] Tafticht T., Agbossou K., Doumbia M. L. and Cheriti A., "An improved maximum power point tracking method for photovoltaic systems". *Renewable Energy*, Vol. 33, No. 7, pp. 1508-1516, July 2008.
- [10] Dasgupta N., Pandey A. and Mukerjee A. K., "Voltage-sensing-based photovoltaic MPPT with improved tracking and drift avoidance capabilities", *Solar Energy Materials and Solar Cells*, Vol. 92, No.12, pp. 1552-1558, December 2008.
- [11] Kuo Y. C., Liang T. J. and Chen J. F., "Novel maximum-power-point tracking controller for photovoltaic energy conversion system". *IEEE Trans. Ind. Electron*, Vol. 48, No. 3, pp. 594-601, Jun. 2001.

- [12] Hussein K. H. and Mota I., "Maximum photovoltaic power tracking: an algorithm for rapidly changing atmospheric conditions", *Generation, Transmission and Distribution, IEE Proceedings*, Vol. 142, No. 1, pp. 59-64, Jan. 1995.
- [13] Yu G. J., Jung Y. S., Choi J. Y. and Kim G. S. "A novel two-mode MPPT control algorithm based on comparative study of existing algorithms", *Solar Energy*, Vol. 76, No. 4, pp. 455-463, April 2004.
- [14] Masoum M. A. S. and Sarvi M., "A new fuzzy-based maximum power point tracker for photovoltaic applications", *Iranian Journal of Electrical & Electronic Engineering*, Vol. 1, No.1, pp. 28-35, January 2005.
- [15] Altas I. H. and Sharaf A. M., "A novel maximum power fuzzy logic controller for photovoltaic solar energy systems", *Renewable Energy*, Vol. 33, No. 3, pp. 388-99, March 2008.
- [16] Duru H. T., "A maximum power tracking algorithm based on $I_{mpp} = f(P_{max})$ function for matching passive and active loads to a photovoltaic generator", *Solar Energy*, Vol. 80, No. 7, pp. 812-822, July 2006.
- [17] Huang B. J., Sun F. S. and Ho R. W., "Near-maximum-power-point-operation (n MPPO) design of photovoltaic power generation system", *Solar Energy*, Vol. 80, No. 8, pp. 1003-1020, August 2006.
- [18] Liu Y. H., Liu C. L., Huang J. W. and Chen J. H., "Neural-network-based maximum power point tracking methods for photovoltaic systems operating under fast changing environments", *Solar Energy*, Vol. 89, pp. 42-53, March 2013.
- [19] Kakosimos P. E. and Kladas A. G., "Implementation of photovoltaic array MPPT through fixed step predictive control technique", *Renewable Energy*, Vol. 36, No. 9, pp. 2508-2514, September 2011.
- [20] Lin C. H., Huang C. H., Yi-Du Y. C. and Chen J. L., "Maximum photovoltaic power tracking for the PV array using the fractional-order incremental conductance method", *Applied Energy*, Vol. 88, No. 12, pp. 4840-4847, December 2011.
- [21] Jiang L. L., Maskell D. L. and Patra J. C., "A novel ant colony optimization-based maximum power point tracking for photovoltaic systems under partially shaded conditions", *Energy and Buildings*, Vol. 58, pp. 227-236, March 2013.
- [22] Mohammadpour A., Mokhtari H. and Zolghadri M. R., "Control of Series Resonant Converter with Robust Performance Against Load and Power Circuit Components Uncertainties", *Iranian Journal of Electrical & Electronic Engineering*, Vol. 5, No. 4, pp. 244-252, Dec. 2009.
- [23] Chu C. C. and Chen C. L., "Robust maximum power point tracking method for photovoltaic cells: A sliding mode control approach", *Solar Energy*, Vol. 83, No. 8, pp. 1370-1378, August 2009.
- [24] Il-Song K., "Robust maximum power point tracker using sliding mode controller for the three-phase grid-connected photovoltaic system", *Solar Energy*, Vol. 81, No. 3, pp. 405-414, March 2007.
- [25] Il-Song K., "Sliding mode controller for the single-phase grid connected photovoltaic system", *Applied Energy*, Vol. 83, pp. 1101-1115, October 2006.
- [26] Charles J.P., Ismail M.A. and Bordure G. "A critical study of the effectiveness of the single and double exponential models for I-V characterization of solar cells", *Solid-State Electron*, Vol. 28, No. 8, pp. 807-820, August 1985.
- [27] Gow J. A. and Manning C. D., "Development of a Photovoltaic Array Model for Use in Power-Electronics Simulation Studies", *IEE Proceedings of Electric Power Applications*, Vol. 146, No. 2, pp. 193-200, March 1999.



Jaber Ghazanfari was born in kerman, Iran, 1985. He received the B.Sc. and M.Sc. degrees from University of Shahid Bahonar, Kerman, Iran in 2010 and 2012. His interests are in the power system control, stability and evolutionary computation.



Malihe Maghfoori Farsangi received her B.Sc. degree in Electrical Engineering from Ferdowsi University, Iran in 1995, and Ph.D. degree in Electrical Engineering from Brunel Institute of Power Systems, Brunel University, UK in 2003. Since 2003, she has been with Kerman University, (Kerman, Iran), where she is currently an Associate Professor of Electrical Engineering. Her research interests

include power system control and stability and computational intelligence.